Supporting Information

Multiomics imaging using high energy H_2O gas cluster ion beam secondary ion mass spectrometry (GCIB-SIMS) of frozen-hydrated cells and tissue

Hua Tian[1], Sadia Sheraz née Rabbani[2], John C. Vickerman[3], Nicholas Winograd[1]

1 Department of Chemistry, Pennsylvania State University, University Park, PA 16802, US; 2 The Rosalind Franklin Institute, Harwell Campus, Didcot, OX11 0FA, UK; 3 Manchester Institute of Biotechnology, University of Manchester, Manchester M1 7DN, UK

Corresponding author: hut3@psu.edu

Table of Contents for Supporting Information

Table S1 Negative ion signal yields from cell lipids as a function of analysis conditions, presented as a ratio compared to the yields obtained using a CO_2 cluster beam on a chemically fixed sample at room temperature. Data in red highlight a very significant enhancement of yield.

	m/z	H_2O beam cryofixed 100K	CO_2 beam cryofixed 100K	H_2O beam GA fixed RT	CO_2 beam GA fixed RT
Fatty acids	255.23	4.91	0.36	4.09	1
	281.25	3.93	0.28	3.59	1
	283.26	3.00	0.66	5.37	1
Intact lipids	673.48	12.24	0.93	11.08	1
	687.51	14.88	0.72	14.90	1
	701.49	15.34	1.26	19.10	1
	747.50	26.00	1.22	11.31	1
	760.52	28.34	4.02	13.19	1
	773.53	40.73	0.79	15.95	1
	788.53	28.33	3.02	17.58	1
	810.50	18.33	0.73	22.01	1
	835.49	3.23	0.27	15.46	1
	847.42	121.11	0.77	14.64	1
	863.53	3.92	0.29	18.21	1
	873.44	34.89	2.40	5.75	1
	885.51	3.19	0.45	24.11	1
Cardiolipins	1403.99	60.14	2.32	13.73	1
	1429.99	118.56	0.67	13.88	1
	1441.93	108.52	5.50	18.08	1
	1455.99	418.94	0.65	29.64	1
	1467.96	509.42	3.26	12.49	1
	1495.98	161.00	4.71	32.05	1

The intensities are averaged from two cell samples from the same batch of culture.

Table S2 Selected ion species and empirical assignments from total negative ion mass spectrum of HeLa cells and mouse brain tissue

***m/z* expr.**	**window Da**	**assignment**	**Formula**	**class**	***m/z* theo.**	**delta ppm**
179.0561	0.02	Glucose [M-H]$^-$	$C_6H_{11}O_6^-$	metabolite	179.0556	3.0
180.0661	0.02	Tyrosine [M-H]$^-$	$C_9H_{10}NO_3^-$	metabolite	180.0661	0.2
191.0197	0.02	Citrate / isocitrate [M-H]$^-$	$C_6H_7O_7^-$	metabolite	191.0192	2.7
241.0125	0.02	Hexosemonophosphate [M-H_2O-H]$^-$	$C_6H_6O_9P^-$	metabolite	241.0113	4.7
255.2336	0.02	FA(C16:0) [M-H]$^-$	$\mathbf{C_{16}}H_{31}O_2^-$	FFA	255.2324	4.8
259.0224	0.02	Hexosemonophosphate [M-H]$^-$	$C_6H_8O_{10}P^-$	metabolite	259.0219	2.0
266.0894	0.02	Adenosine [M-H]$^-$	$C_{10}H_{12}N_5O_4^-$	metabolite	266.0889	1.8
281.2480	0.02	FA(C18:1) [M-H]$^-$	$\mathbf{C_{18}}H_{33}O_2^-$	FFA	281.2481	-0.3
282.0272	0.02	N-acetylglucosaminephosphate [M-H_2O-H]$^-$	$C_8H_{13}NO_8P^-$	metabolite	282.0379	-37.8
283.2637	0.02	FA(C18:0) [M-H]$^-$	$\mathbf{C_{18}}H_{35}O_2^-$	FFA	283.2631	1.9
300.0489	0.02	N-acetylglucosamine-1 or 6-phosphate [M-H]$^-$	$C_8H_{15}NO_9P^-$	metabolite	300.0484	1.5
303.2332	0.02	FA(C20:4) [M-H]$^-$	$C_{20}H_{31}O_2^-$	FFA	303.2324	2.5
306.0760	0.02	GSH [M-H]$^-$	$C_{10}H_{16}N_3O_6S^-$	metabolite	306.076	0.1
309.2785	0.02	FA(C20:1)	$C_{20}H_{35}O_2^-$	FFA	309.2794	-2.8
327.2331	0.02	FA(C22:6) [M-H]$^-$	$C_{22}H_{31}O_2^-$	FFA	327.2324	2.2
328.0500	0.02	cAMP [M-H]$^-$	$C_{10}H_{11}N_5O_6P^-$	metabolite	328.0447	16.2
346.0558	0.02	AMP [M-H]$^-$	$C_{10}H_{13}N_5O_7P^-$	metabolite	346.0553	1.6
527.9561	0.02	ATP [M+Mg-3H]$^-$	$C_{10}H_{13}N_5O_{13}P_3Mg^-$	metabolite	527.9573	-1.9
673.4797	0.05	unidentified		unidentified		
687.5246	0.05	unidentified		unidentified		
701.5140	0.05	PA(36:1) [M-H]$^-$	$C_{39}H_{72}O_8P^-$	PA	701.5121	2.7
747.5002	0.05	PA(40:6) [M-H]$^-$	$C_{43}H_{72}O_8P^-$	PA	747.4964	5.1
760.5202	0.05	PS(34:1) [M-H]$^-$	$C_{40}H_{76}NO_{10}P$	PS	760.5128	9.7
773.5301	0.05	PG(36:2) [M-H]$^-$	$C_{42}H_{78}O_{10}P^-$	PG	773.5332	-4.0
788.5418	0.05	PS(36:1) [M-H]$^-$	$C_{42}H_{79}NO_{10}P^-$	PS	788.5431	-1.6
810.5257	0.05	PS(38:4) [M-H]$^-$	$C_{44}H_{77}NO_{10}P^-$	PS	810.5274	-2.1
834.5262	0.05	PS(40:6) [M-H]$^-$	$C_{46}H_{77}NO_{10}P^-$	PS	834.5274	-1.4
835.5310	0.05	PI(34:1) [M-H]$^-$	$C_{43}H_{80}O_{13}P^-$	PI	835.5337	-3.2
838.5537	0.05	PS(40:4) [M-H]$^-$	$C_{46}H_{81}NO_{10}P^-$	PS	838.5587	-6.0
847.4256	0.05	unidentified		unidentified		
863.5635	0.05	PI(36:1) [M-H]$^-$	$C_{45}H_{84}O_{13}P^-$	PI	863.565	-1.7
873.5520	0.05	unidentified		unidentified		
885.5493	0.05	PI(38:4) [M-H]$^-$	$C_{47}H_{82}O_{13}P^-$	PI	885.5487	0.6
888.5642	0.05	PS 44:7 [M-H]$^-$	$C_{50}H_{84}NO_{10}P^-$	PS	888.5754	-12.6
1403.9901	0.1	CL(68:2) [M-H]$^-$	$C_{77}H_{145}O_{17}P_2^-$	CL	1403.9956	3.9
1429.9903	0.1	CL(70:5) [M-H]$^-$	$C_{79}H_{143}O_{17}P_2^-$	CL	1425.9801	21.5
1441.9362		unidentified		unidentified		
1447.9678	0.1	CL(72:8) [M-H]$^-$	$C_{81}H_{141}O_{17}P_2^-$	CL	1447.9644	-2.5
1455.9946	0.1	CL(72:4) [M-H]$^-$	$C_{81}H_{149}O_{17}P_2^-$	CL	1456.0275	-22.6
1467.9622	0.1	unidentified		unidentified		
1495.9812	0.1	CL(76:12) [M-H]$^-$	$C_{85}H_{141}O_{17}P_2^-$	CL	1495.9643	11.3
1873.8992	0.1	GT3 44:1 [M-H]$^-$	$C_{89}H_{158}N_4O_{37}^-$	Ganglioside	1874.0526	-8.2

Supplementary figures

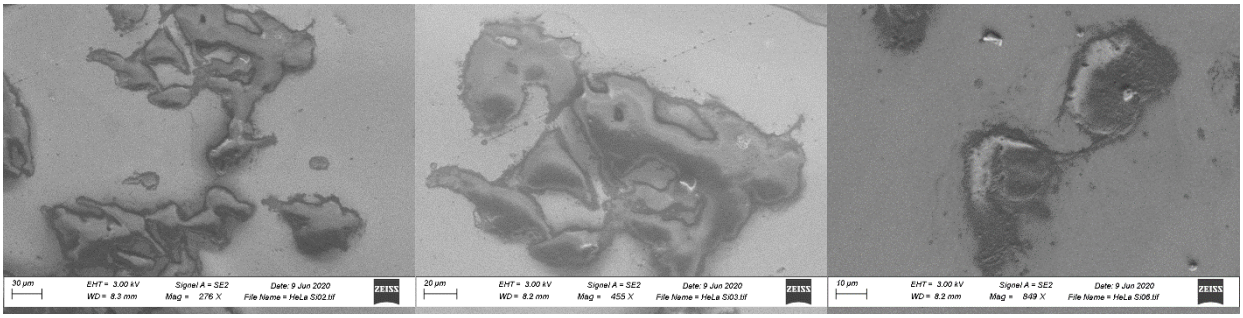

Figure S1 CryoSEM images of HeLa cells cultured on the Si wafer and prepared by plunging into liquid ethane and then the liquid nitrogen. The images at 276×, 455× and 848× show that the cells have been preserved properly without lysing or burst. The cellular morphology and sizes are consistent with the microscopy images published in the literature.

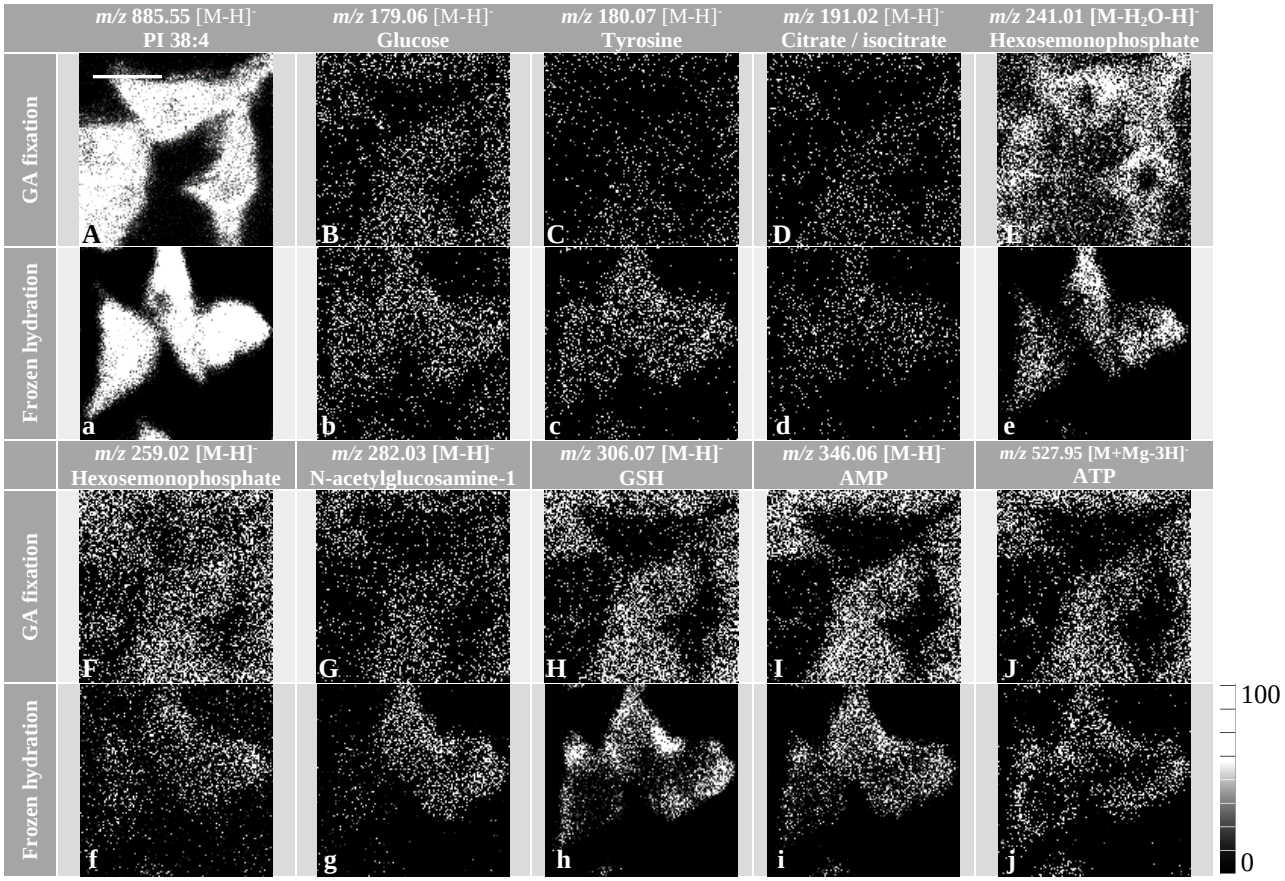

Figure S2 Selected metabolites and lipid ion images acquired using 70 keV $(H_2O)_{28k}$ with varying sample preparations, (A-J) GA fixed, RT; (a-j) Frozen-hydrated, 110K. The lipid ion PI (38:4) at *m/z* 885.55 outlines the cellular region as in A and a. In the GA fixed cells, the metabolites in B-J are mainly localized outside of the cellular region. On the contrary, the same metabolites in b-j are localized within the cellular region in the frozen-hydrated cells. Scale bar is 50 µm. The gray scale bar indicates the ion intensity.

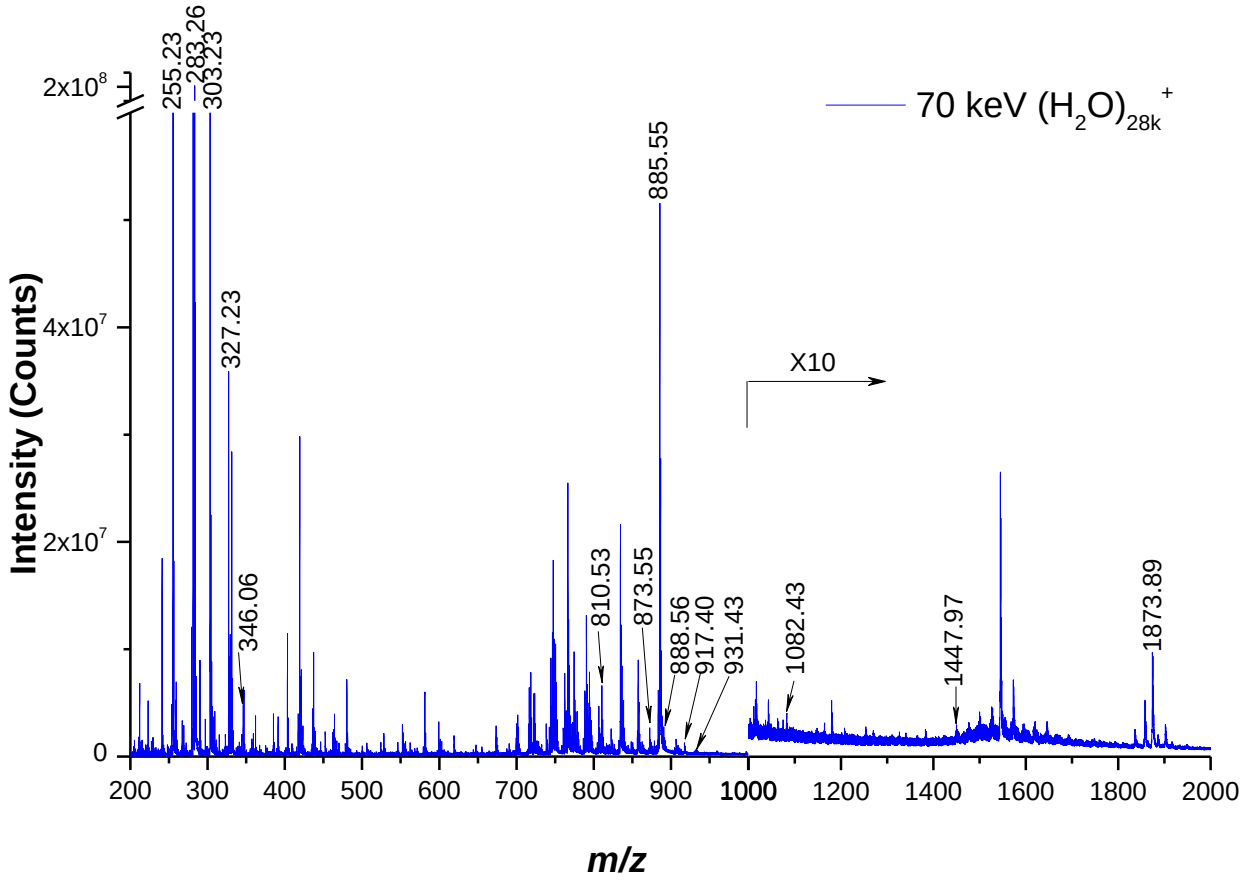

Figure S3 Mass spectrum of mouse brain tissue using 70 KeV $(H_2O)_{28k}^+$.

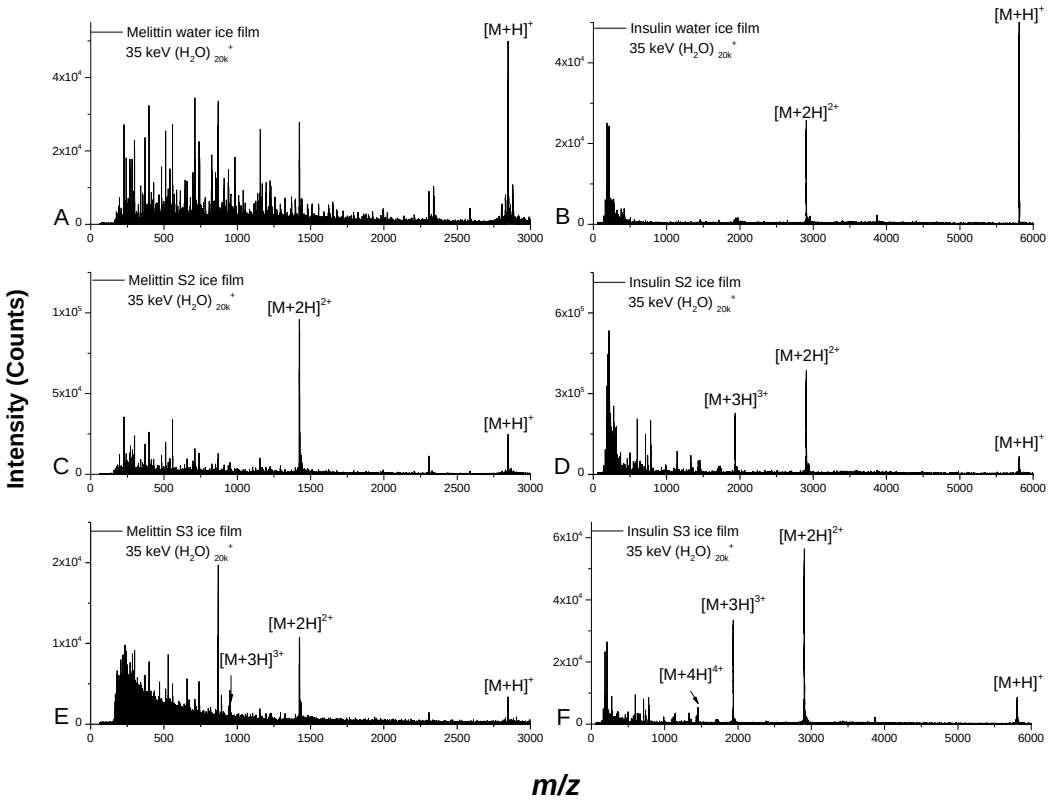

Figure S4 Positive spectra of melittin and insulin using 35 keV $(H_2O)_{20k}^+$ at water ice film in A and B, Lesa plus 1% HCl ice film in C and D, and 3-NBN in ACN solution ice film in E and F. It is clearly seen that more acidity will enhance doubly charged molecular ion as in C and D, 3-NBN promotes triple charged molecular ion as in E and F.

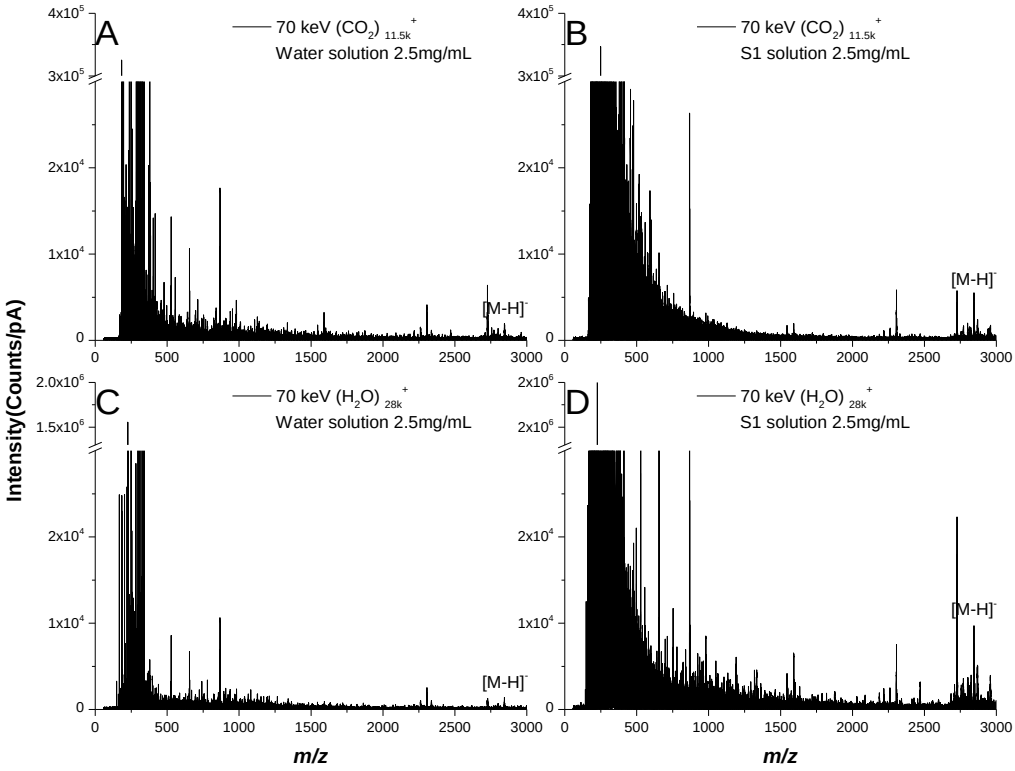

Figure S5 Negative spectra of melittin acquired at -100K with different conditions, A, Spin coated film using 70 keV $(CO_2)_{11.5k}^+$; B, Ice film using 70 keV $(CO_2)_{11.5k}^+$; C, Spin coated film using 70 keV $(H_2O)_{28k}^+$; D, Ice film using 70 keV $(H_2O)_{28k}^+$. Peptide does not favor negative ionization, however water beam enhance $[M-H]^-$ by 2 times compared with condition B, while 4.5 times compared with condition A.

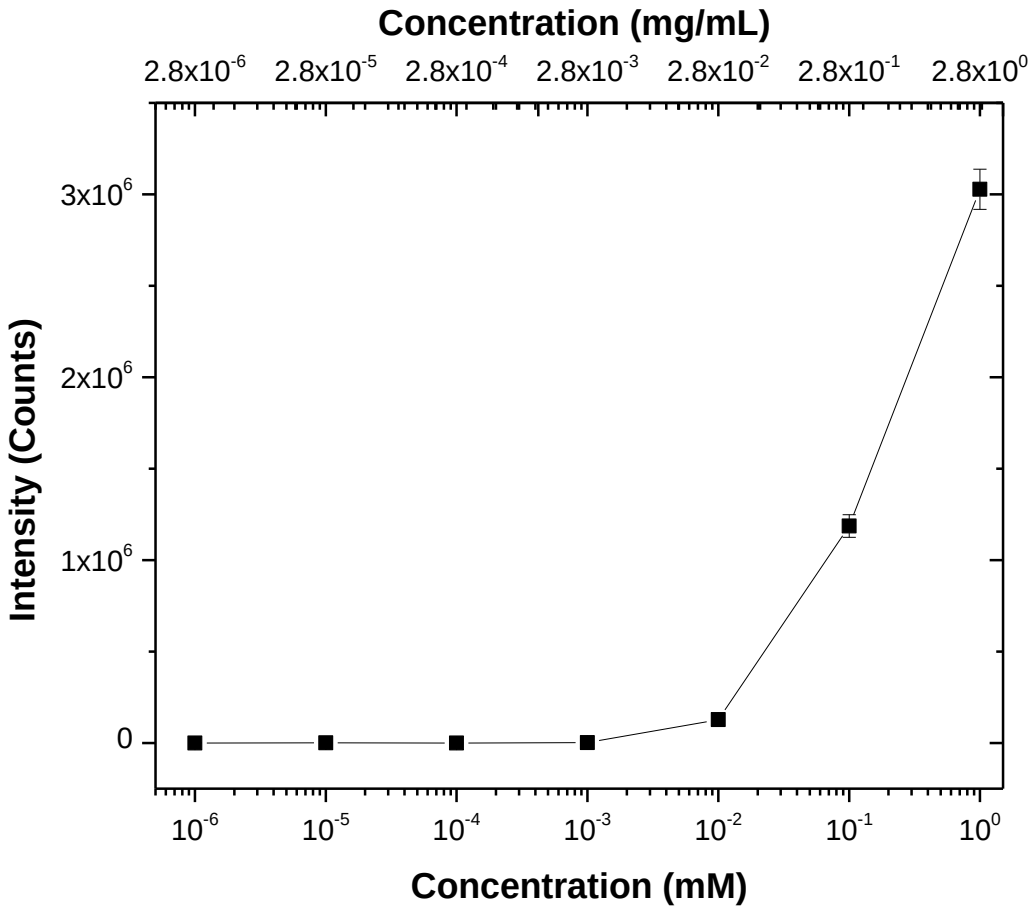

Figure S6 Detection limit of melittin using 70 keV $(H_2O)_{28,000}^+$. The plot of signal level along with varying concentrations indicates that the detection limit of melittin is approx. 10 µM.